Electro-optical characterization of photovoltaic devices

Author: Martí Busquets Masó.
Facultat de Física, Universitat de Barcelona, Diagonal 645, 08028 Barcelona, Spain.

Advisors: Sergi Hernández Márquez *and* Julià López Vidrier

Abstract: In this work, we adapted and improved a commercial system designed to measure the *external quantum efficiency* (EQE) and the *internal quantum efficiency* (IQE) of commercial solar cells. With this purpose, we controlled and synchronized a monochromator and a *semiconductor device analyser* Agilent B1500A in order to perform different electro-optical measurements being able to measure very low current signals ($\sim 10^{-13}A$). To verify that the system was working correctly, we used a Si solar cell whose fill factor, efficiency and spectral response are tabulated. Furthermore, we used this experimental setup to study a Si-NCs/SiO_2 superlattice system deposited on a *p*-type silicon substrate. In this study, we characterized the $I(V)$ curve of the devices in dark and under white light illumination. We measured the spectral response and IQE of devices containing different NC sizes. IQE of ∼14.2 - 20.5 were achieved in the 850-1000 nm wavelength range, and a shift of the IQE edge to higher energies was observed when decreasing the NC size, demostrating electro-optical quantum confinement.

I. INTRODUCTION

The project was divided in to two parts:
In the first part we adapted and improved a commercial system designed to measure the *external quantum efficiency* (EQE) and the *internal quantum efficiency* (IQE) of commercial solar cells. We achieved the control of the different elements of the system [Bentham PVE300 monochromator and Agilent B1500A *semiconductor device analyser* (SDA)] and synchronization of them by using Matlab in MatlabGUI interface [1]. We created a panel in which the user can perform different kinds of measurements (intensity as a function of voltage, spectral response...) and data processing. Furthermore, the system is adapted in order to reduce the noise level to be able to measure small current signals ($\sim 10^{-13}A$). Finally, we execute different measurements in a Si solar cell, whose spectral response is tabulated, in order to verify that the system is well programmed and works correctly.

The second part consists of the study of the electro-optical properties of Si-NC/SiO_2 supperlattice devices deposited on *p*-type silicon substrate using the previous developed setup. In fact, Si NCs can improve the optical absorption efficiency in respect to bulk silicon due to the electronic quantum confinement of the electron wavefunction inside the quantum dots (QDs). Moreover, Si NCs present a bandgap energy that can be tuned by controlling the Si NC size [2]. One of the potential applications of this kind of systems are all-Si tandem solar cells [3], due to the combination of different bandgaps achieved by different NC sizes, which can increase virtually the solar cell efficiency up to 85% [4]. In this work, we focus the research in the optoelectric conversion of Si-NC/SiO_2 systems. Due to the fact that these devices are in an early stage of optimization, the electro-optical conversion is expected to be poor, and a high-sensitive experimental setup is needed to evaluate their electrical response. Using this developed setup we were able to determine the spectral response, EQE and IQE of Si-NC/SiO_2 supperlattices for different NC sizes.

II. EXPERIMENTAL DETAILS

A. Sample and device details

Prior to the study of the NC-based devices, the equipment modification and control was checked by means of a calibrated commercial Si cell, whose spectral response in the studied range and photovoltaic parameters are well known [5].

The Si NC devices under study alternate silicon-rich silicon oxynitride (SRON) and stoichiometric silicon dioxide (SiO_2) superlattices (SLs) [2], which were deposited on wet chemically cleaned *p*-type (100)-Si substrates (B-doped, with a base resistivity of 1-20 Ω·cm) by plasma-enhanced chemical-vapor deposition (PECVD). In these samples the thickness of the SiO_2 barrier layer (t_{SiO_2}) was held constant at 1 nm (the optimum achievable thickness for efficient electron conduction [6]), whereas the SRON layer thickness (t_{SRON}) was varied

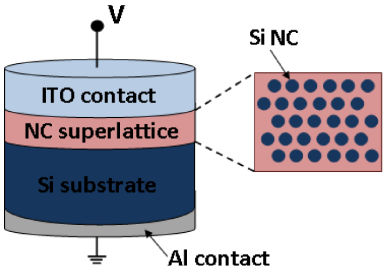

FIG. 1: (Left) Sketch of the NC-based devices studied in this work: Si NC/SiO_2 superlattices with ITO and Al contacts on top and bottom, respectively. (Right) Cross-section scheme of the superlattice structure. Lengths are not to scale.

with values of 2.5, 3.5 and 4.5 nm. The total number of deposited bilayers was five, the total nominal thicknesses therefore being 17.5, 22.5 and 27.5 nm, respectively. In all samples, the stoichiometry of the SRON layer was kept constant at $SiO_{0.93}N_{0.23}$, which corresponds to a Si excess of 17 at. %, according to [Si]=$(1-0.5x-0.75y)/(1+x+y)$, x and y being the [O]/[Si] and [N]/[Si] ratios, respectively [7]. In order to precipitate and crystallize the Si excess inside the SRON layers, the samples were annealed at 1150°C for 1 h in a high purity N_2 atmosphere. To prevent the oxidation of the layers close to the surface, a 10 nm SiO_2 layer was deposited on top of the structure before the annealing process. After the annealing treatment, this oxide layer was etched in precisely controlled, highly diluted HF without overetching into the Si NC layer. Further details about the sample deposition can be found elsewhere [8]. Finally, using a photolithographic pattering, a 70 nm layer of indium tin oxide (ITO) was deposited on the top of the devices and, on the bottom of the p-type Si substrate, a full-area Al sputtering was carried out. The Fig. 1 shows a sketch of the device.

B. Electro-optical measurements

In the Electronics Department of the Univ. of BCN, we have a commercial system designed to measure the *external quantum efficiency* (EQE) and the *internal quantum efficiency* (IQE) of commercial solar cells. Furthermore, the system has a quartz lamp that simulates the solar spectrum. On one hand, it consists of one monochromator (with two diffraction gratings) coupled to two lamps (xenon and halogen lamps). The system uses a different lamp and diffraction grating depending on the wavelength that has to be applied. On the other hand, we used two high resolution probes, connected to an Agilent B1500A SDA by means of triaxial cables, in order to measure the electrical response of the devices either in dark or under illumination conditions. In addition, devices are placed on a thermal chuck that permits a good electrical contact and allows controlling the temperature in the range from 10 to 60°C.
Furthermore, the system has a bias lamp that reproduces the solar power. Its intensity on the devices can be controlled by means of a mechanical slit. Nevertheless, the bias lamp does not reproduce the whole solar spectrum (especially the UV-blue range).

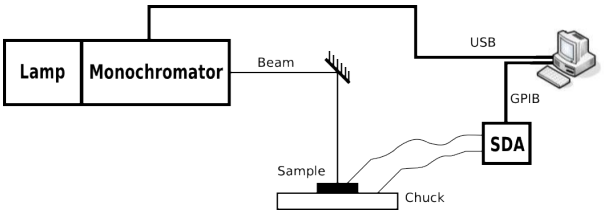

FIG. 2: Scheme of the experimental system after the synchronization.

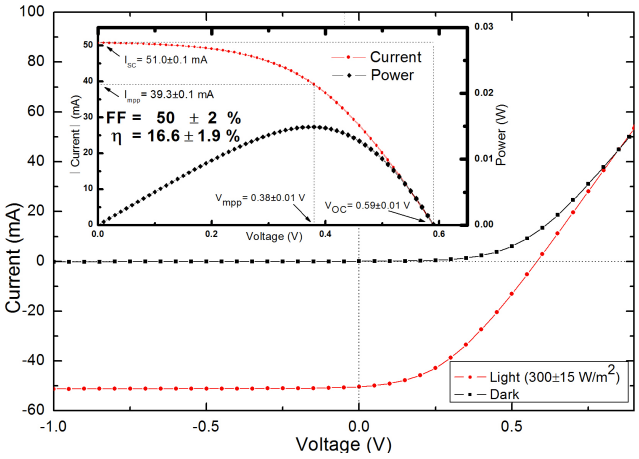

FIG. 3: Si solar Cell I(V) characteristics in dark and white light illumination. The inserted graph show the calculation of solar cell efficiency by I(V) under white light illumination. The white light illumination in both graphics is 300±15 W/m^2, and the illuminated area is 300±10 mm^2.

Before the use of SDA, the commercial system could only realise measurements with a maximum resolution of 10^{-6}A. After the implementation and computer control of the SDA, we are able to do different kinds of measurements with a resolution up to 10^{-13}A.

The light intensity emitted by the system (lamp plus monochromator) changes with the wavelength. So, to normalize the spectrum obtained with the system we needed to do one additional measurement, after every spectrum acquisition, with a calibrated photodiode, in order to normalize the spectrum of the sample for the incident optical power. The final program can do this normalization automatically. The user merely needs to introduce the spectrum of the sample, the spectrum of the photodiode and the photodiode calibration.

III. RESULTS AND DISCUSSION

A. Setup improvements and new functionalities

A userfriendly interface using Matlab 2012 has been created that controls each system of the experimental setup. Fig. 2 shows a scheme of the experimental system after the synchronization via computer. The different measurements that the system can perform are: intensity as a function of voltage ($I-V$), intensity as a function of the incident wavelength (spectral response), $I-V$ for different wavelength (3D map: intensity-voltage-wavelength), intensity as a function of time ($I-t$) and high time resolution $I-t$. In the case of the $I-t$ the user can change the wavelength or voltage during the measurement. The limit time precision of the high time resolution $I-t$ was 1 ms [9].

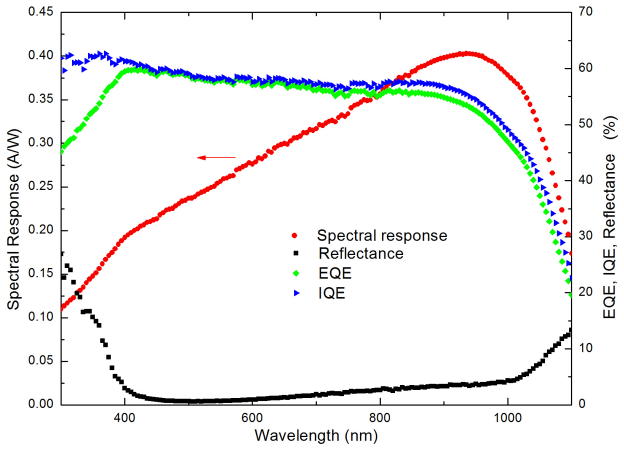

FIG. 4: Si solar cell spectral response, reflectance, EQE and IQE, at 0V.

B. System verification: Commercial Si solar cell

To verify the implementation done within the first part, we realized different measurements with a calibrated Si solar cell to verify that the system was well programmed and worked correctly. The first measurement consisted in the study of the intensity as a function of voltage. Furthermore, we calculated the fill factor (FF) and the efficiency (η) of the solar cell under illumination, using Eq. (1) and (2), respectively.

$$FF = 100 \times \frac{V_{mpp} \times J_{mpp}}{V_{oc} \times J_{sc}} \tag{1}$$

$$\eta = 100 \times \frac{P_{el,out}}{P_{op,in}} = 100 \times \frac{V_{mpp} \times J_{mpp}}{P_{op,in}} \tag{2}$$

where V_{mpp} and J_{mpp} are the voltage and current density, respectively, at the maximum power point, whereas V_{oc} and J_{sc} are the open-circuit voltage and short-circuit current density, respectively. $P_{el,out}$ states for the total electrical output power, while $P_{op,in}$ is the total optical input power (i.e. the solar power).

The maximum intensity permitted, in order not to damage the system (current compliance), is about 50 mA. If we apply the power equivalent to the solar spectrum (1000 W/m^2) the current of the solar cell is higher than this current compliance. Thus, to carry out this measurement, we reduced the power of the light radiation (closing the lamp slit) until the current at 0 V is about 50 mA. To be able to calculate the efficiency we measured the optical power under these conditions with a power meter. The measured optical power was 300±15 W/m^2. The obtained curves are represented in Fig. 3. We obtained a $I_{sc} = 51.0 \pm 0.1$mA, $V_{oc} = 0.59 \pm 0.01$ V, $I_{mpp} = 39.3 \pm 0.1$ mA, $V_{mpp} = 0.38 \pm 0.01$V, $FF = 50 \pm 2\%$ and efficiency of 16.6±1.9 % [using Eq. (1) and (2)]. The measured parameters of the solar cell are in good accordance with the reference values provided by the manufacturer [5].

On the other hand, we performed a measurement of intensity as a function of wavelength (spectral response, SR) at 0V in order to compare it with the reference response. Fig. 4 shows the SR of the Si solar cell. The SR is directly correlated with the EQE (Eq. 3). SR and EQE can hinder a direct correlation with the physical mechanisms because it does not consider the light reflected (R) by the sample, which does not contribute to the generated current. So, we need to evaluate the IQE (Eq. 4).

$$EQE = \frac{\phi_{electrons}}{\phi_{incidentphotons}} = SR \times \frac{hc}{\lambda q_e} \tag{3}$$

$$IQE = \frac{\phi_{electrons}}{\phi_{absorbedphotons}} = \frac{EQE}{1-R} \tag{4}$$

where ϕ is the flux, λ is the wavelength, q_e is the electron charge, h is the Planck's constant and c is the speed of light in vacuum. Again, the SR concord with the reference SR provided by the manufacturer (not shown)[5].

C. Si NCs devices

Fig. 5 shows the current as a function of voltage in dark and under bias illumination for Si-NCs devices. We have the bottom contact (Al) grounded and the top contact (ITO) connected to a potential (V) swept from -9V to 9V.

In the accumulation region ($V < 0$), and in dark conditions, a large current is carried by electrons that tunnel the SiO_2 barrier from the ITO contact to the QDs

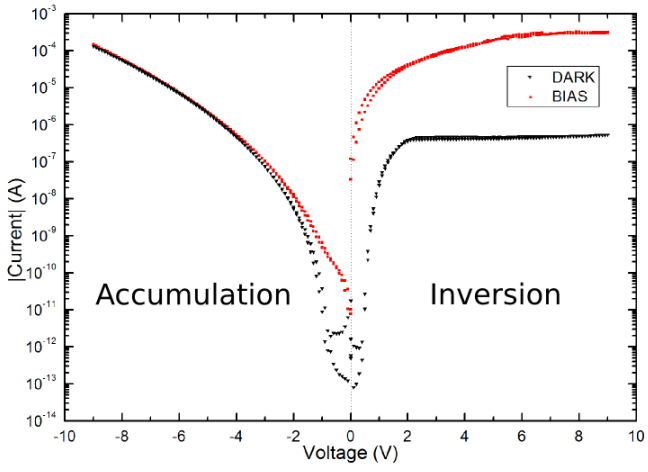

FIG. 5: I(V) in dark and under white light illumination for Si-NCs devices with Si NC sizes of 3.5 nm in the accumulation and inversion region.

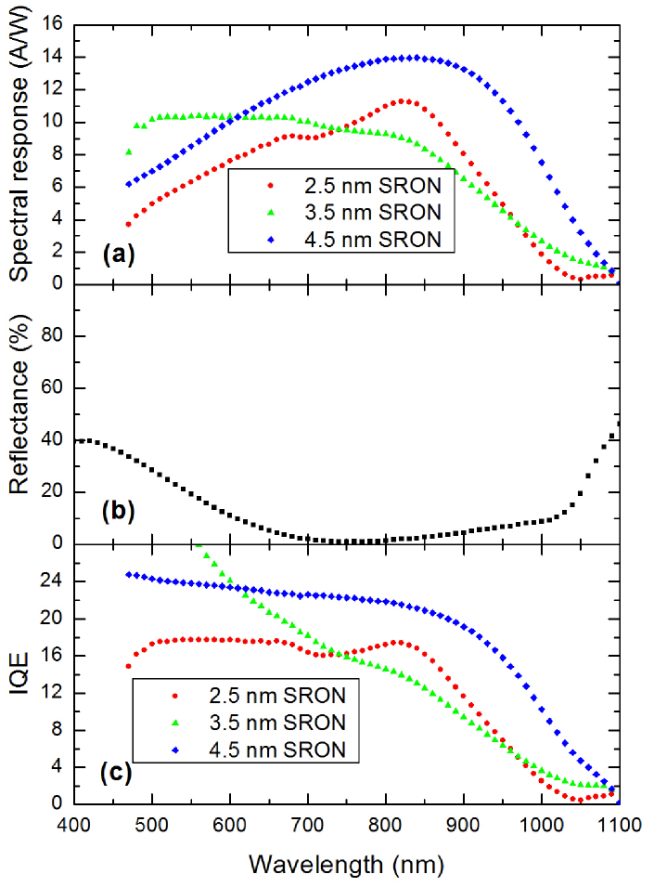

FIG. 6: Spectral response (a), reflectance (b) and IQE (c) of Si-NCs devices Si NC sizes ranged from 2.5 nm to 4.5 nm. Spectral response and IQE are performed at 8V (inversion region).

and holes that tunnel the SiO_2 barrier from the p-type Si substrate to the QDs. An electron and hole accumulation appears in the ITO and p-type Si substrate, respectively, and the electron and hole concentrations increase rapidly with the voltage as the effective tunneling barrier decreases in both cases. Under white light illumination, the current remains practically similar because $\Delta n \ll n$ (where Δn is the carrier density photogenerated and n is the carrier density in dark conditions). On the other hand, in the inversion region ($V > 0$), and in dark conditions, a low current appears because electrons are tunneling the SiO_2 barrier from the p-type Si to the QDs, and this conduction is limited due to the density of electrons in the p-type Si substrate (electrons are the minority carriers). In this case, under white light illumination, there is a strong increase current by a factor of $> 10^2$ because $\Delta n \gg n$ (see Fig. 5). Similar $I(V)$ behaviour was reported for Ge QDs embedded in SiO_2 matrix [10].

Fig. 6(a) displays the spectral response of Si NCs at 8 V (inversion region) for the devices containing NC sizes of 2.5, 3.5 and 4.5 nm, obtained by measuring the current under illumination (for each wavelength), and subtracting the dark current at the given voltage, afterwards normalizing for the incident optical power. We obtained a responsivity of 14.0 A/W at 840 nm for Si NC size of 4.5 nm and 11.3 A/W and 9.0 A/W at 820 nm for Si NC sizes of 2.5 and 3.5 nm, respectively. The spectral response may be affected by the light reflected from the systems, which does not contribute to the generated current. To take this under consideration, we needed to calculate the internal quantum efficiency (IQE) by measuring the reflectance (R) at normal incidence [Fig. 6 (b)], and then normalize by the number of absorbed photons, $AbsorbedPhotons = (1-R) \times IncidentPhotons$, for each given wavelength. The IQE of the devices is represented in Fig. 6(c), which shows a maximum IQE of 20.5, 14.2 and 17.8 around 800-900 nm, for Si NC sizes of 4.5, 3.5 and 2.5 nm, respectively [see Fig. 6(b)]. The IQE edge is shifted towards high energies in comparison to bulk Si (see Fig. 4) for all Si NC devices: in the bulk Si we have the photocondutivity edge around 1000-1100 nm while in the case of Si NCs it is around 850-1050 nm. Furthermore, there is a blue shift in the IQE edge depending on the Si NC size: the IQE edge energy increases when the Si NC size decreases. Actually, when reducing the Si NCs size their energy levels are modified, due to the quantum confinement effect, according to the effective mass approximation (EMA). The discrete solutions for the confined energy levels are given by $\Delta E_n = \frac{\pi^2\hbar^2}{2m^*a^2} \cdot n^2$ [11], where $\hbar = h/2\pi$ is the reduced Planck's constant, m^* is effective mass of the carriers, a is the NC diameter and n is the energy level. So, when the NC size decreases, the energy of the levels, i.e. their bandgap energy, increases. Therefore, the energy of the bandgap in first approximation is given by Eq. (5):

$$E_{g,SiNCs}(a) = E_{g,Si} + \frac{B}{a^2} \tag{5}$$

where $E_{g,Si}$ is the bandgap of the bulk material, B is a coefficient that depends on m^* and a is the QD diameter. In the real Si-NC we have a non-infinite confining barrier potential, so this approximation becomes inaccurate for small crystal diameters.

In order to determine the bandgap energy of the NCs devices, we used the IQE edge. We obtained band gaps of 1.32, 1.29 and 1.24 eV for the 2.5, 3.5 and 4.5 nm NC size, respectively. In Fig. 7 we compare these results with the equation of confined energy states of the NC (Eq. 5), electroluminescence (EL) measurements of identical Si NC-based devices [12] and different photoluminescence (PL) measurements of Si NCs reported in different publications (see ref. [13], [14] and [15]). Finally, the bandgap energy of the devices calculated by the IQE edge is lower than the EL and PL peaks. This is because in the devices we have a contribution of the Si substrate that can not be avoided. The effective Si NC-bulk Si system presents an intermediate bandgap energy that therefore decreases with respect to the expected bandgap for NCs (obtained from PL and EL).

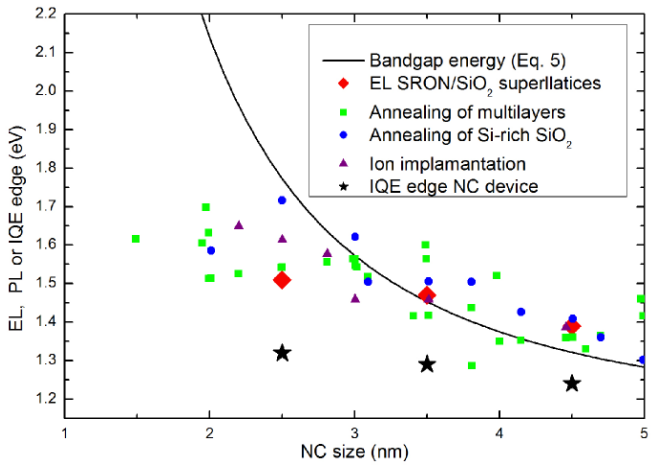

FIG. 7: Summary of different publications reporting photoluminescence (PL) peaks and IQE edge of the studied NCs devices as a function of Si NC size. Reported results on EL of SI-NCs/SiO_2 multilayers [12], PL of Si NCs obtained from SRON multilayer annealing [13], PL of annealing of Si-rich SiO_2 [14] and PL of ion-implanted NCs [15] are displayed for the sake of comparison.

IV. CONCLUSIONS

In summary, in the first part we developed a commercial system to measure small signals. We are now able to measure signals of $\sim 10^{-13}$A and we can carry out different kinds of measurements with the new controlling program. Furthermore, we checked that the program is working correctly by carrying out different measurements using a calibrated Si solar cell.

In the second part, the Si-NC/SiO_2 superlattices deposited on *p*-type Si substrate with ITO (front) and Al (back) contacts, present an IQE of 20.5 at 890 nm, 14.2 at 820 nm and 17.8 at 840 nm for the Si NC sizes of 4.5, 3.5 and 2.5 nm, respectively. Furthermore, we observed a blue shift in the IQE edge of the latter devices in comparison to bulk Si. The IQE edge increases when the Si NCs size decreases, which confirms quantum confinement. Finally, we compare these results with the equation of confined energy estates and EL and PL peaks of Si NC-based devices reported in different publications. We obtained a bandgap of 1.32, 1.29, 1.24 eV for the 2.5, 3.5 and 4.5 nm NC size, respectively. The IQE edge energy is lower than the EL and PL peaks because in the devices we have a contribution of the Si substrate that can not be avoided. The effective Si NC-bulk Si system presents an intermediate bandgap energy that therefore decreases with respect to the expected bandgap for NCs. We will work in the future to be able to systematically get rid of this contribution by separately evaluating it.

Acknowledgments

I would like to express my specially gratitude to Dr. Sergi Hernández and PhD student Julià López for introducing me in the world of research, helping me at every time and give me their support as well as the whole group. Also to Prof. Blas Garrido to give me the opportunity to work in his electro-photonics group and Prof. M. Zacharias for providing us the devices.

Finally, I would also like to thank my family and friends, who as always helped me, but specially to my mother, who always gave me her support all the time.

[1] Matlab 2008, *MathWorks*, Natick, Massachusetts, USA.
[2] Zacharias, *et al.*, Appl. Phys. Lett. **80**, 661 (2002).
[3] G. Conibeer, *et al.*, Thin Solid Films **511-512**, 654-662 (2006).
[4] P. Wurfel, *Physics of Solar Cells: From Basic Principles to Advanced Concepts*, 2nd edition (2009), Wiley (New York).
[5] 6″ *Mono-Crystalline Silicon Solar Cell (3 busbar, Alkali): V03*, Solarmade^{TM} (*www.solarmade.com*).
[6] S. Gutsch, *et al.*, J. Appl. Phys. **113**, 133703 (2013).
[7] S. Hernández, *et al.*, J. Appl. Phys. **103**, 064309 (2008).
[8] A. M. Hartel, *et al.*, Thin Solid Films **520**, 121-125 (2011).
[9] "Agilent B1500A/B1505A Device Analyzer Series, Programming Guide." (Edition 10).
[10] S. Cosentino, *et al.*, Appl. Phys. Lett. **98**, 221107 (2011).
[11] P.Y. Yu, M.Cardona, Fundamentals of Semiconductors, 4th edition (2010), Springer (Berlin).
[12] J. López-Vidrier, *et al.*, J. Applied Physics. **114**, 163701 (2013).
[13] G. Conibeer, *et al.*, Thin Solid Films **511-512**, 654 (2006); M. Zacharias, *et al.*, Appl. Phys. Lett. **80**, 611 (2002); S. Kim, *et al.*, J. Nanomater **2012**, 572746 (2012); L. Khriachtchev, *et al.*, J. Phys.: Condens. Matter **16**, 3219 (2004); L. X., *et al.*, Appl. Phys. Lett. **81**, 4248 (2002); X. Yu, *et al.*, J. Non-Cryst. Solids **357**, 3524 (2011); M. Cazzanelli, *et al.*, J. Appl. Phys. **96**, 3164 (2004); X. J. Hao, *et al.*, Nanotechnology **20**, 485703 (2009); H. Rinnert, *et al.*, J. Appl. Phys. **106**, 023501 (2009); A. M. Hartel, *et al.*, Phys. Rev. B **85**, 165306 (2012).
[14] S. Takeoka, *et al.*, Phys. Rev. B **62**, 16820 (2000); X. X. Wang, *et al.*, Phys. Rev. B **72**, 195313 (2005); K. Matsuhisa, *et al.*, J. Lumin **132**, 1157 (2012); W. D. A. M. de Boer, *et al.*, Nat. Nanotechnol. **5**, 878 (2010); Y. Lebour, *et al.*, Physica E **41**, 990 (2009).
[15] S. Guha, J. Appl. Phys. **84**, 5210 (1998); L. Pavesi, *et al.*, Nature **408**, 440 (2000); G. A. Kachurin, *et al.*, Nanotechnology **19**, 355305 (2008); O. Korotchenkov, *et al.*, J. Appl. Phys. **111**, 063501 (2012).